Tapered Block Copolymers Containing Ethylene and a Functionalized Comonomer

Steve J. Diamanti, Vikram Khanna, Atsushi Hotta, Robert C. Coffin, Diane Yamakawa, Edward J. Kramer, Glenn H. Fredrickson, and Guillermo C. Bazan*

Institute for Polymers and Organic Solids and Mitsubishi Chemical Center for Advanced Materials, Departments of Chemistry, Materials, and Chemical Engineering, University of California, Santa Barbara, California 93106

Received November 16, 2005; Revised Manuscript Received February 26, 2006

ABSTRACT: We report the synthesis of tapered block copolymers of ethylene with 5-norbornen-2-yl acetate (**1**) by the nickel catalyst system [*N*-(2,6-diisopropylphenyl)-2-(2,6-diisopropylphenylimino)propanamide] Ni(η^1-CH_2Ph)(PMe_3) (**2**) and $Ni(COD)_2$ (bis(1,4-cyclooctadiene)nickel). This technique utilizes a one-pot semibatch copolymerization in which ethylene is continuously added while **1** is depleted by incorporation into the polymer chain. The simplicity of this technique allows the construction of a polymer library, which enabled us to study the effect of polymer composition and chain length on solid-state morphology and mechanical and thermal properties. From these studies we were able to derive a profile relating the probability of **1** insertion vs degree of polymerization (X_n). Under proper experimental conditions, these tapered polymers form ordered microphase-separated morphologies where the phase morphology is modulated by the polymer chain length. The percent crystallinity and storage modulus of the polymers were found to be chain length dependent.

Introduction

Self-assembling systems are becoming a viable method for achieving nanoscale feature sizes and high feature fidelity, which find use in various applications.[1,2] Block copolymers are ideal molecules for achieving such organization due to their thermodynamically controlled driving force to nanoscale ordering.[3,4] As a result of advances in the methods of polymer synthesis, it is possible to "program" nanoscale morphologies and sizes through control of experimental conditions and polymer composition.[5−8] Uses of such block copolymer templates have appeared, particularly in nanoimprinting.[9,10] In addition to controlling the morphologies and length scales of self-assembly by synthetic conditions, it would be advantageous to tailor the physical and mechanical properties of these polymer domains.

Gradient, or tapered, copolymers have a chemical structure with a gradual change of composition along the polymer chain, from one comonomer to the other.[11,12] If the average chain length is sufficiently long, the degree of incompatibility between the two monomers is high and the gradient profile provides chain ends that contain mainly one type of monomer, then microphase-separated structures similar to those observed in traditional block copolymers can be observed.[13] This special class of gradient copolymers, called tapered block copolymers (TBCs), are of importance; in particular, they are efficient compatibilizers of polymer blends and may be superior to block copolymers for this application.[14−16] The phase morphology and interfacial energy in TBCs are modulated by the length and sharpness of the composition gradient.[17−21]

Living polymerization methods are required for the synthesis of gradient structures, since to achieve similar average composition drifts in each polymer chain, all chains must be initiated simultaneously and must participate in the propagation sequence until the end of the reaction.[15] Because of this requirement, gradient copolymers have been synthesized primarily by controlled radical polymerization[22−26] and anionic polymerization[27−34] methods. Tapered polymer structures containing ethylene and functionalized comonomers have not existed previously,[35] primarily because of the limited options for living polymerization initiators.[36−41] Such materials could make a substantial impact in designing blends of polyethylene and polar engineering plastics[42] because the polarity gradient along their chain would reduce the interfacial energy and lead to better mixing.

In this contribution we disclose the synthesis, characterization, and bulk properties of TBCs containing ethylene and the polar comonomer 5-norbornen-2-yl acetate (**1**). Our technique is a remarkably simple method, involving a one-pot synthesis with no need for sequential monomer addition. Furthermore, we show that the structure and composition of the gradient copolymers can be controlled with variation of the initial concentration of the polar comonomer. As a result, the mechanical properties of these TBCs can be tailored at the synthesis stage.

Results and Discussion

Synthesis and Characterization. The initiator system generated with (L^iPr_2)Ni(η^1-CH_2Ph)(PMe_3) (**2**) [(L^iPr_2) = *N*-(2,6-diisopropylphenyl)-2-(2,6-diisopropylphenylimino)propanamide] and 2.5 equiv of $Ni(COD)_2$ (bis(1,5-cyclooctadiene)-nickel)[43] shows "quasi-living"[44] characteristics for the copolymerization of ethylene and **1** (Figure 1). It occurred to us that a semi-batch reaction whereby the ethylene pressure is kept constant and the concentration of **1** is allowed to deplete by incorporation into the polymer structure would lead to the desired tapered structure. Under these circumstances, the growing chain is rich in **1** at the start of the reaction. As the reaction proceeds, [**1**] decreases, leading to an increase in the fraction of ethylene incorporated into the chain. The final structure of the polymer was anticipated to have a polar amorphous terminus (rich in **1**) and a nonpolar, semicrystalline chain (primarily polyethylene) on the other end. The overall procedure is technically simple. A reactor is initially filled with a solution of the initiator mixture and **1** (see Figure 1). Polymerization

* To whom correspondence should be addressed. E-mail: bazan@chem.ucsb.edu.

10.1021/ma052456c CCC: $33.50
Published on Web 03/29/2006

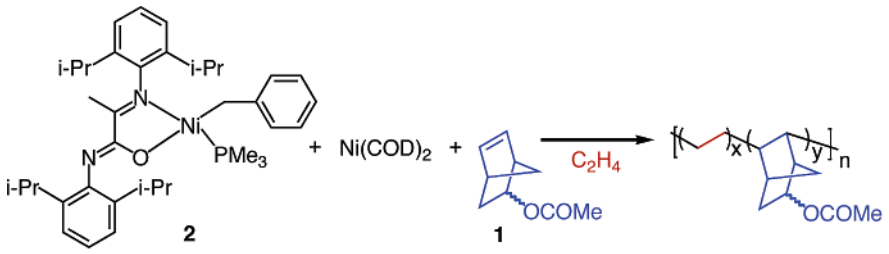

Figure 1. Gradient copolymerization method. The ratio *x*/*y* increases as a function of *n*. The gradient bar illustrates the compositional variation from segments rich in **1** (blue) to segments rich in C_2H_4 (red).

Table 1. Summary of Polymerization Reactions[a]

entry	reaction time (min)	M_n (kg/mol)	PDI	mol % **1**
1	4	10 ± 1	1.3	18 ± 1
2	5	18 ± 1	1.2	18 ± 1
3	8	27 ± 2	1.2	14 ± 1
4	10	28 ± 1	1.3	14 ± 1
5	20	37 ± 3	1.4	12 ± 1
6	25	47 ± 3	1.4	11 ± 1
7	35	55 ± 5	1.4	10 ± 1
8	45	63 ± 3	1.3	9 ± 1
9	60	94 ± 10	1.5	6 ± 1
10	80	109 ± 1	1.5	6 ± 1
11	100	136	1.6	5 ± 1
12	120	170	1.5	4 ± 1

[a] Conditions: $P_{C_2H_4}$ = 200 psi, [**1**] = 0.15 M, [**2**] = 0.67 mM, [Ni(COD)$_2$] = 1.67 mM, in toluene. Each entry shows the average from three polymerizations, except for entries 11 and 12. Mol **% 1** is calculated by ^{1}H NMR spectroscopy. Molecular weight determinations were measured by gel permeation chromatography (GPC) against universal calibration from polystyrene standards.

takes place when ethylene is added and is terminated after a chosen reaction time.

Table 1 summarizes a set of polymerization reactions where the ethylene pressure was kept constant at 200 psi. Examination of Table 1 shows that there is a progressive increase in average molecular weight with reaction time, even up to 120 min. This increase is consistent with the quasi-living characteristics of the polymerization reaction. Ideal living characteristics are not achieved due to reaction variables such as the varying levels of incorporation of **1** into the copolymer chain and the precipitation of the product after 45 min of reaction time. Copolymers with larger fractions of **1** are soluble in toluene, whereas the ethylene-rich segments formed at later stages of the reaction have poor solubility in toluene. Table 1 also shows that the overall fraction of **1** in the product decreases with longer reaction times. The chains thus have the highest fraction of **1** at the beginning, when [**1**] is at its maximum.

Two additional sets of tapered copolymers were prepared starting with lower and higher initial $[\mathbf{1}]_0$ values (0.075 and 0.225 M). Figure 2 shows the decrease of the average content of **1** in the polymer chain with increasing molecular weight as a function of the initial $[\mathbf{1}]_0$. Since **1** is consumed solely through incorporation into the polymer, the quantity of unreacted **1** can be calculated from the structural composition according to eq 1:

$$\mathbf{1}_0 - W_{\mathbf{1}} M_p = \mathbf{1}_x \qquad (1)$$

In eq 1, $\mathbf{1}_0$ is the initial comonomer mass, $W_{\mathbf{1}}$ is the weight fraction of **1** in the product, M_p is the mass of isolated polymer, and $\mathbf{1}_x$ is the mass of **1** remaining in solution. After 60 min, under the reaction conditions listed in Table 1, greater than 99%

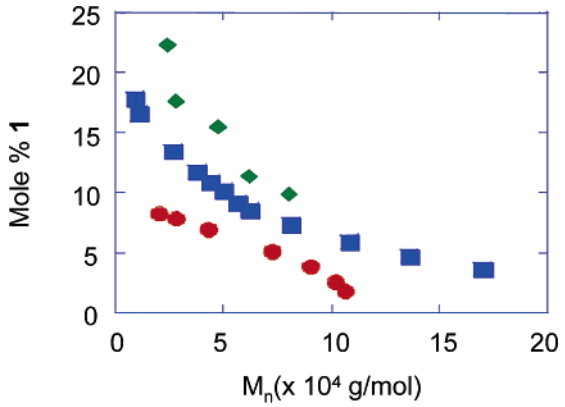

Figure 2. Molar percentage of **1** in the polymer chain as a function of molecular weight and initial $[\mathbf{1}]_0$, where the data for $[\mathbf{1}]_0$ = 0.075, 0.150, and 0.225 M are given by circles (red), squares (blue), and diamonds (green), respectively. The polymer series with $[\mathbf{1}]_0$ = 0.225 M could not be extended beyond M_n = 80 kg/mol due to gel formation in the reactor.

of $\mathbf{1}_0$ has been incorporated into the growing chains. Extension of the polymer chain from this point onward takes place predominantly by polyethylene formation. As displayed in Figure 2, by controlling $[\mathbf{1}]_0$, one can create a variety of polymer compositions.

Figure 2 provides the average content of **1** vs M_n; however, it does not make clear information on the instantaneous composition as a function of chain length. For a more complete picture of the tapered structure it would be useful to know the probability of **1** insertion as the reaction proceeds. Obtaining this information typically requires continuous monitoring of both molecular weight and structural composition vs time, which is not possible in our laboratories. However, the data in Table 1 may be used for an estimate. Consider for example two consecutive entries (a and b) in Table 1. The probability of **1** insertion in the interval between the two entries ($P_{\mathbf{1}a\rightarrow b}$) can be estimated by

$$P_{\mathbf{1}a\rightarrow b} = [(F_{\mathbf{1}b}X_{nb}) - (F_{\mathbf{1}a}X_{na})]/(X_{nb} - X_{na})$$

where $F_{\mathbf{1}b}$, X_{nb}, $F_{\mathbf{1}a}$, and X_{na} are the molar fraction of **1** in entry b, the average degree of polymerization in entry b, the fraction of **1** in entry a, and the average degree of polymerization in entry a, respectively. The average number of **1** at a given X_n is provided by $F_{\mathbf{1}}X_n$. The X_n for each entry is obtained by dividing the number-average molecular weight (M_n) by the average mass of the monomer units (M_{avg}).[45] We use $M_{\mathbf{1}}F_{\mathbf{1}} + M_E F_E$ to obtain M_{avg}, where $M_{\mathbf{1}}$, $F_{\mathbf{1}}$, M_E, and F_E are the molecular weight of **1**, the molar fraction of **1** in the chain, the molecular weight of ethylene, and the molar fraction of ethylene in the chain, respectively.

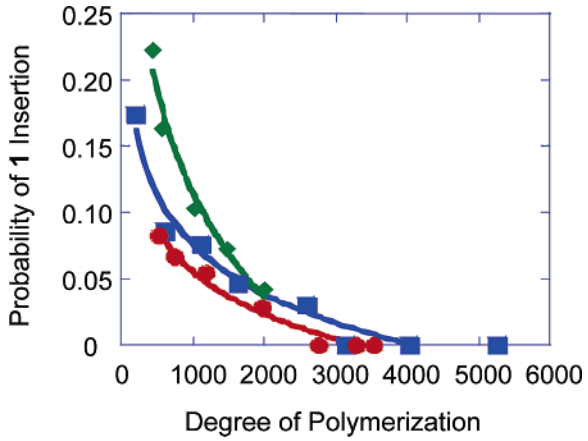

Figure 3. Plot of $P_{1a\rightarrow b}$ against X_n. $[1]_0 = 0.075$, 0.15, and 0.225 M are shown in circles (red), squares (blue), and diamonds (green), respectively. The lines are a guide to the eye.

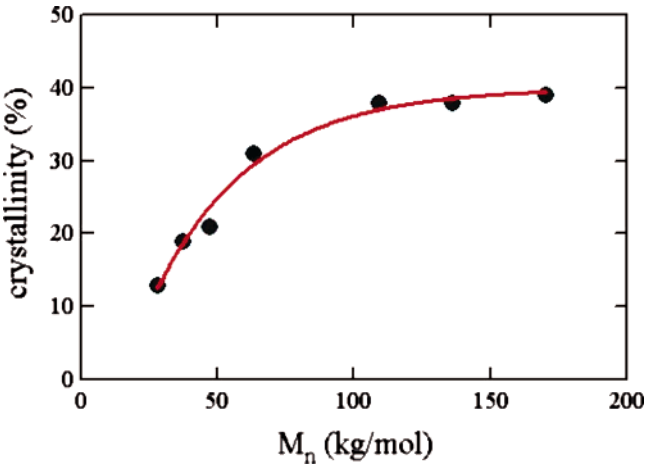

Figure 4. Crystallinity vs number-average molecular weight. The line is a guide to the eye.

Figure 3 shows how $P_{1a\rightarrow b}$ changes as a function of X_n at three values of $[1]_0$. Higher $[1]_0$ causes steeper tapering profiles and higher initial incorporation of **1** into the polymer chain. The steep tapering profile leads to a polymer that changes rapidly from a polar amorphous segment to a nonpolar polyethylene-like segment. For the lowest $[1]_0$ the $P_{1a\rightarrow b}$ profile leads to a polymer that transforms more gradually from a semipolar amorphous segment to polyethylene. Ultimately, the $P_{1a\rightarrow b}$ profile gives an estimate of the instantaneous incorporation of **1** into the copolymer at different chain lengths, and these estimates can be used to create structures with desired composition and tapering profile.

Solid-State Characterization and Properties. The crystallinities of the TBCs, as measured by differential scanning calorimetry (DSC), are in agreement with the profile in Figure 3. Figure 4 shows a plot of the percent crystallinity (Table 1, entries 4−12) vs M_n. The lowest molecular weight entries with the highest **1** content (Table 1, entries 1−3) have no measurable crystallinity. For $M_n > 100$ kg/mol, the polyethylene crystallinity saturates at ∼40%, a value that corresponds well to that for the polyethylene obtained with this initiator system. Note that for $[1]_0 = 0.15$ M Figure 3 shows that the three longest polymer segments have $P_{1a\rightarrow b} = 0$; thus. the chain ends of the three longest polymers are essentially polyethylene.

The $P_{1a\rightarrow b}$ profile in Figure 3 shows that for $[1]_0 = 0.15$ M the instantaneous composition of the copolymer chain tapers from nearly 20 mol % **1** to polyethylene for polymers with $M_n > 100$ kg/mol. This difference in composition gradient led us to expect phase separation in the solid state.[48] The products listed in Table 1 were examined by transmission electron microscopy (TEM). No indication of phase separation was observed for polymers with $M_n < 63$ kg/mol (reaction time < 45 min). As shown in Figure 5A, a lamellar morphology, where semicrystalline PE layers (light) alternate with amorphous copolymer layers, is observed for a polymer with $M_n = 63$ kg/mol (Table 1, entry 8). For the products obtained after longer reaction times, the morphology changes from alternating lamellar sheets to a less organized phase (Figure 5B), in which the polyethylene-rich segments form the matrix and the **1**-rich block forms smaller, cylindrical-like domains. While the tapered structure of the products allows us to create microphase-separated

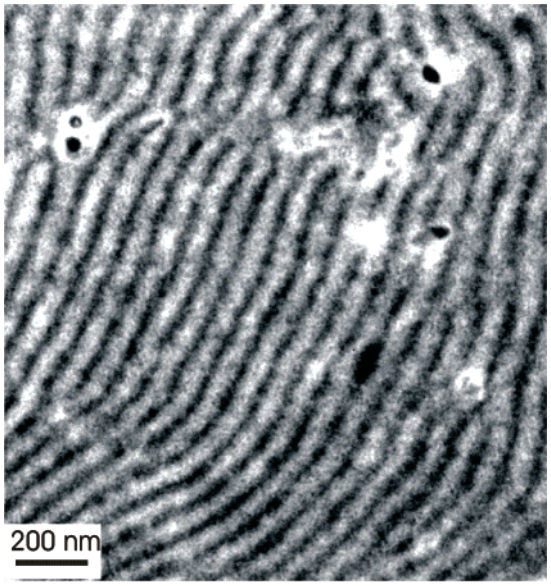

A

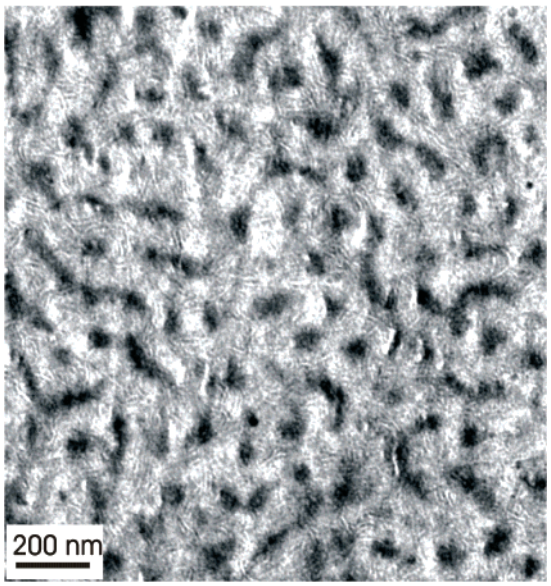

B

Figure 5. (A) Transmission electron micrograph (TEM) of Table 1, entry 8 ($M_n = 63$ kg/mol). The morphology is lamellar, where semicrystalline PE layers (light) alternate with amorphous copolymer layers. The dark spots are caused by stain contamination by RuO_4. (B) TEM of Table 1, entry 12 ($M_n = 170$ kg/mol). The morphology is a poorly organized hexagonal phase, where amorphous copolymer cylinders are embedded in a semicrystalline PE matrix (light). PE crystals can also be observed in the matrix.

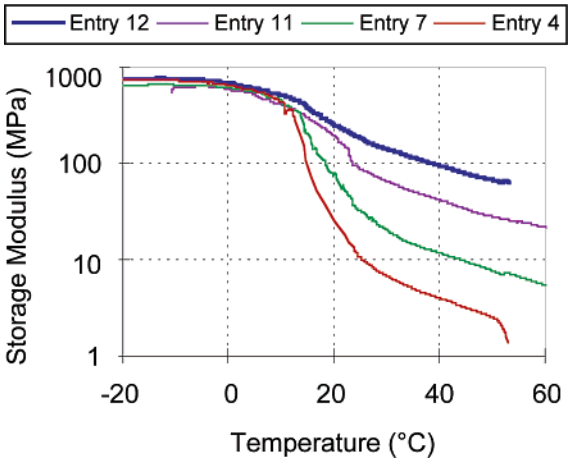

Figure 6. Dynamic mechanical testing on tapered copolymers showing the results of the storage modulus. Entry numbers in the legend correspond to polymers in Table 1.

structures whose morphologies are a function of polymer chain length, there are limitations. For example, it is not possible to create short gradient copolymers that order into microphase-separated morphologies. This is due to the finite chain length needed for the polymer to taper from a segment rich in **1** to a sufficiently incompatible polyethylene sequence.

Since crystallinity changes as a function of M_n, we anticipated mechanical properties that are chain length dependent. Tension film geometry was used to investigate the storage modulus G' as a function of temperature (Figure 6). At lower temperatures (below the T_g) the storage moduli of all these samples are nearly the same, while at elevated temperatures the moduli shift to higher values for higher M_n polymers. This is primarily due to the fact that increasing chain length leads to longer segments of polyethylene and correspondingly higher levels of polyethylene crystallinity. Additionally, the change from a lamellar morphology at lower M_n, where the stiff polyethylene domains alternate with the amorphous **1**-rich domains, to a morphology at the highest M_n, in which the stiff polyethylene domain forms a continuous matrix, may account for part of the chain length dependent mechanical properties. These results indicate that since the molecular weight grows nearly linearly with reaction time, the storage modulus (and thus mechanical properties) can be altered through control of this experimental variable.

Conclusion

In summary, we developed a simple one-step methodology for the synthesis of tapered block copolymers containing ethylene and a polar comonomer that show microphase-separated structures and chain length dependent mechanical properties. Furthermore, the thermal, GPC, and ^{1}H NMR characterization along with TEM examination and mechanical testing support our proposal of a structure with an initial, amorphous, **1**-rich segment that tapers to a highly crystalline polyethylene segment. The ease of this synthetic method allows us to create libraries of tapered copolymers with varying molecular weights and **1** content. It is interesting to note that **1** exists as a mixture of *endo* and *exo* isomers, which may have different reactivities and rates of incorporation into the polymer chain.[38,46] The exact tapered profile could indeed be quite complex. Despite these uncertainties, the information we have gained from the tapering profile at different $[\mathbf{1}]_0$ values yields guidelines for the creation of materials with tailored bulk properties. We are currently extending this synthetic methodology toward the creation of multiblock tapered copolymers to explore the effect of multiblock architecture on microphase separation and mechanical, physical, and thermal properties.

Experimental Section

General Remarks. All manipulations were performed under an inert atmosphere using standard glovebox and Schlenk techniques. All reagents were used as received from Aldrich, unless otherwise specified. A Parr 100 mL metal reactor (model 4565) was used for all polymerizations. Ethylene was purchased from Matheson Tri-Gas (research grade, 99.99% pure) and was purified by passage through high-pressure, stainless steel, oxygen and moisture traps (Matheson models OT-4-SS and MT-4-SS). Toluene, THF, hexane, and pentane were distilled from benzophenone ketyl. Toluene for polymerization runs was distilled from sodium/potassium alloy. 5-Norbornen-2-yl acetate (**1**) was purchased from Aldrich and was vacuum-distilled before use. [*N*-(2,6-Diisopropylphenyl)-2-(2,6-diisopropylphenylimino)propanamide]Ni(η^1-CH_2Ph)(PMe_3) (**2**) and Ni$(COD)_2$ were synthesized as reported previously[47] and purified by recrystallization.

Typical Tapered Copolymerization of Ethylene and 5-Norbornen-2-yl Acetate; $[\mathbf{1}]_0 = 0.15$ M. A typical copolymerization is performed as follows. Inside a glovebox a metal reactor was loaded with **2** (20 μmol, 31.6 mg), Ni$(COD)_2$ (50 μmol, 27.6 mg), **1** (4.50 mmol, 0.685 g), and toluene such that the final volume of this solution was 30 mL. The metal reactor was sealed inside the glovebox and was attached to a vacuum/nitrogen line manifold. Ethylene was fed continuously into the reactor at 200 psi, and the pressurized reaction mixture was stirred at 20 °C. Ethylene was vented after a specific reaction time, and acetone was added to quench the polymerization. The precipitated polymer was collected by filtration and dried under high vacuum overnight.

Polymer Characterization. NMR spectra were obtained using Varian Unity 400 or 500 spectrometers. ^{1}H NMR spectra of the polymers were obtained in mixed solvent (C_6D_6/1,2,4-trichlorobenzene 1:4 ratio in volume) at 115 °C. Gel permeation chromatography (GPC) measurements were performed on a Polymer Labs high-temperature GPC system (model PL-220). Differential scanning calorimetry was used to determine the thermal characteristics of the copolymers using a TA Instruments DSC 2920. The DSC measurements were recorded during the second heating/cooling cycle in the −10 to 180 °C range at a rate of 5 °C/min. Each sample for DSC was approximately 5−10 mg. The crystallization temperature (T_c), the melting point (T_m), and the heat of fusion (H_m) of the materials were determined in this way. Dynamic mechanical analysis was performed using a TA Instruments 2980 DMA. Tension film geometry was used to investigate the storage modulus G' as a function of temperature and to detect the glass transition of the samples by measuring tan δ. The typical size of the measured samples was approximately 7 mm in length, 1.5 mm in width, and 0.15 mm in thickness. Both cooling and heating processes were performed at 3 °C/min for each sample. Applied frequency was 1 Hz, and applied deformation ranges from 10 to 50 μm (i.e., applied strain ranges from ∼0.15 to ∼0.7, well within the linear region of the materials) depending on the softness of the materials.

Transmission electron microscopy studies were performed on annealed copolymer films. Bulk polymer samples were annealed in high vacuum for 1 day at 200 °C, followed by 3 days at 160 °C to allow the microphase to equilibrate, followed by a rapid quench in <1 min to liquid nitrogen temperatures. First the sample surface was cut at −190 °C to make a smooth surface for the stain to penetrate into the sample. The sample was then stained in the vapor of a 0.5% RuO_4 stabilized aqueous solution (Electron Microscopy Science) for a period of 5 days. Sections of the stained polymers 80 nm thick were then cut using a Leica Ultracut UCT ultramicrotome with a diamond knife at room temperature. TEM images of the stained samples were obtained using a FEI Tecnai G2 Sphera TEM operating at 200 kV. The observed contrast is due to the local oxidation of the amorphous phase of the block copolymer by RuO_4.

Acknowledgment. The authors are grateful to Mitsubishi Chemical−Center for Advanced Materials (MC−CAM) and the

Department of Energy (DE-FG03098ER 14910) for financial support and to Dr. Masatoshi Takagi and Dr. Akio Tanna. This work made use of MRL Central Facilities supported by the MRSEC Program of the National Science Foundation under Award DMR00-80034.

References and Notes

(1) Hadjichristidis, N.; Pispas, S. *Block Copolymers: Synthetic Strategies, Physical Properties, and Applications*; Wiley-Interscience: Hoboken, NJ, 2003.
(2) Cohen, R. E. *Curr. Opin. Solid State Mater. Sci.* **2000**, *4*, 587−590.
(3) Bates, F. S.; Fredrickson, G. H. *Annu. Rev. Phys. Chem.* **1990**, *41*, 525−557.
(4) Klok, H. A.; Lecommandeux, S. *Adv. Mater.* **2001**, *13*, 1217−1229.
(5) Patten, T. E.; Matyjaszewski, K. *Acc. Chem. Res.* **1999**, *32*, 895−903.
(6) Hawker, C. J.; Bosman, A. W.; Harth, E. *Chem. Rev.* **2001**, *101*, 3661−3668.
(7) Hadjichristidis, N.; Pitsikalis, M.; Pispas, S.; Iatrou, H. *Chem. Rev.* **2001**, *101*, 3747−3792.
(8) Coates, G. W.; Hustad, P. D.; Reinartz, S. *Angew. Chem., Int. Ed.* **2002**, *41*, 2236−2257.
(9) Cheng, J. Y.; Mayes, A. M.; Ross, C. A. *Nat. Mater.* **2004**, *3*, 823−828.
(10) Lazzari, M.; Lopez-Quintela, M. A. *Adv. Mater.* **2003**, *15*, 1583−1594.
(11) Kryszewski, M. *Polym. Adv. Technol.* **1998**, *9*, 244−259.
(12) Matyjaszewski, K.; Ziegler, M. J.; Arehart, S. V.; Greszta, D.; Pakula, T. *J. Phys. Org. Chem.* **2000**, *13*, 775−786.
(13) Kryszewski, M. *Polym. Adv. Technol.* **1998**, *9*, 244−259.
(14) Fayt, R.; Jerome, R.; Teyssie, P. *J. Polym. Sci., Polym. Phys. Ed.* **1982**, *20*, 2209−2217.
(15) Harrats, C.; Fayt, R.; Jerome, R.; Blacher, S. *J. Polym. Sci., Part B: Polym. Phys.* **2003**, *41*, 202−216.
(16) Harrats, C.; Fayt, R.; Jerome, R. *Polymer* **2002**, *43*, 863−873.
(17) Lefebvre, M. D.; Olvera de la Cruz, M.; Shull, K. R. *Macromolecules* **2004**, *37*, 1118−11123.
(18) Laurer, J. H.; Spontak, R. J.; Smith, S. D.; Ashraf, A.; Buoni, D. J.; Lipscomb, G. G. *Polym. Prepr. (Am. Chem. Soc., Div. Polym. Chem.)* **1994**, *35*, 657−658.
(19) Shull, K. R. *Macromlecules* **2002**, *35*, 8631−8639.
(20) Aksimentiev, A.; Holyst, R. *J. Chem. Phys.* **1999**, *111*, 2329−2339.
(21) Hodrokoukes, P.; Floudas, G.; Pispas, S.; Hadjichristidis, N. *Macromolecules* **2001**, *34*, 650−657.
(22) Neugebauer, D.; Matyjaszewski, K. *Polym. Prepr. (Am. Chem. Soc., Div. Polym. Chem.)* **2003**, *44*, 508−509.
(23) Buzin, A. I.; Pyda, M.; Costanzo, P.; Matyjaszewski, K.; Wunderlich, B. *Polymer* **2002**, *43*, 5563−5569.
(24) Greszta, D.; Matyjaszewski, K. *Polym. Prepr. (Am. Chem. Soc., Div. Polym. Chem.)* **1996**, *37*, 569−570.
(25) Mignard, E.; Leblanc, T.; Bertin, D.; Guerret, O.; Reed, W. F. *Macromolecules* **2004**, *37*, 966−975.
(26) Gray, M. K.; Nguyen, S. T.; Zhou, H.; Torkelson, J. M. *Polym. Prepr. (Am. Chem. Soc., Div. Polym. Chem.)* **2002**, *43*, 112−113.
(27) Asai, S. *Polym. Prepr. (Am. Chem. Soc., Div. Polym. Chem.)* **1996**, *37*, 706−707.
(28) Moctezuma, S. A.; Martinez, E. N. *Polym. Prepr. (Am. Chem. Soc., Div. Polym. Chem.)* **1996**, *37*, 637−638.
(29) Hashimoto, T.; Tsukahara, Y.; Tachi, Y.; Kawai, H. *Macromolecules* **1983**, *16*, 648−657.
(30) Cunningham, R. E. *J. Appl. Polym. Sci.* **1978**, *22*, 2907−2913.
(31) Ishizu, K.; Sunahara, K.; Asai, S. *Polymer* **1998**, *39*, 953.
(32) Sardelis, K.; Michels, H. J.; Allen, G. *Polymer* **1984**, *25*, 1011−1019.
(33) Sardelis, K.; Michels, H. J.; Allen, G. *Polymer* **1987**, *28*, 244−250.
(34) Yu, G. E.; Mistry, D.; Ludhera, S.; Heatley, F.; Attwood, D.; Booth, C. *J. Chem. Soc., Faraday Trans. 1* **1997**, *93*, 3383−3390.
(35) Fujita, M.; Coates, G. W. *Macromolecules* **2002**, *35*, 9640−9647.
(36) Mecking, S.; Johnson, L. K.; Wang, L.; Brookhart, M. *J. Am. Chem. Soc.* **1998**, *120*, 888−899.
(37) Younkin, T. R.; Connor, E. F.; Henderson, J. I.; Freidrich, S. K.; Grubbs, R. H.; Bansleben, D. A. *Science* **2000**, *287*, 460.
(38) Connor, E. F.; Younkin, T. R.; Henderson, J. I.; Hwang, S.; Grubbs, R. H.; Roberts, W. P.; Litzau, J. J. *J. Polym. Sci., Part A: Polym. Chem.* **2002**, *40*, 2842.
(39) Benedikt, G. M.; Elce, E.; Goodall, B. L.; Kalamarides, H. A.; McIntosh, L. H., III; Rhodes, L. F.; Selvy, K. T.; Andes, C.; Oyler, K.; Sen, A. *Macromolecules* **2002**, *35*, 8978−8988.
(40) Matthew, J. P.; Reinmuth, A.; Swords, N.; Risser, W. *Macromolecules* **1996**, *29*, 2755−2763.
(41) Goodall, B. L.; McIntosh, L. H.; Rhodes, L. F. *Macromol. Symp.* **1995**, *89*, 421.
(42) Goretzky, R.; Fink, G. *Macromol. Chem. Phys.* **1999**, *200*, 881.
(43) Diamanti, S. J.; Ghosh, P.; Shimizu, F.; Bazan, G. C. *Macromolecules* **2003**, *36*, 9731−9735.
(44) A reviewer suggested that the term "controlled polymerization" is better suited for these types of reactions.
(45) We recognize the inherent error built in as a result of obtaining M_n, and therefore X_n, from GPC results relative to polystyrene standards. Furthermore, the tapered structures are likely to lead to a complex dependence between hydrodynamic volume and M_n.
(46) Mehler, C.; Risse, W. *Makromol. Chem., Rapid Commun.* **1992**, *13*, 455.
(47) Lee, B. Y.; Bazan, G. C.; Vela, J.; Komon, Z. J. A.; Bu, X. H. *J. Am. Chem. Soc.* **2001**, *123*, 5352.

MA052456C